The single-crystal elastic properties of the jadeite-diopside solid solution and their implications for the composition-dependent seismic properties of eclogite

MING HAO^{1,*}, CAROLINE E. PIEROTTI^{1,2}, SERGEY TKACHEV³, VITALI PRAKAPENKA³, AND JIN S. ZHANG^{1,4,*}

¹Department of Earth and Planetary Sciences, University of New Mexico, 221 Yale Boulevard NE, Albuquerque, New Mexico 87131, U.S.A.

²Albuquerque High School, 800 Odelia Road NE, Albuquerque, New Mexico 87102, U.S.A.

³GeoSoiEnviroCARS, University of Chicago, Argonne National Laboratory, Argonne, Illinois 60439, U.S.A.

⁴Institute of Meteoritics, University of New Mexico, 221 Yale Boulevard NE, Albuquerque, New Mexico 87131, U.S.A.

ABSTRACT

The 13 single-crystal adiabatic elastic moduli (C_{ij}) of a C2/c jadeite sample close to the ideal composition (NaAlSi₂O₆) and a natural P2/n diopside-rich omphacite sample have been measured at ambient condition by Brillouin spectroscopy. The obtained C_{ij} values for the jadeite sample are: $C_{11} = 265.4(9)$ GPa, $C_{22} = 247(1)$ GPa, $C_{33} = 274(1)$ GPa, $C_{44} = 85.8(7)$ GPa, $C_{55} = 69.3(5)$ GPa, $C_{66} = 93.0(7)$ GPa, $C_{12} = 84(1)$ GPa, $C_{13} = 66(1)$ GPa, $C_{23} = 87(2)$ GPa, $C_{15} = 5.4(7)$ GPa, $C_{25} = 17(1)$ GPa, $C_{35} = 28.7(6)$ GPa, $C_{46} = 14.6(6)$ GPa. Voigt-Reuss-Hill averaging of the C_{ij} values yields aggregate bulk modulus $K_S = 138(3)$ GPa and shear modulus G = 84(2) GPa for jadeite. Systematic analysis combing previous single-crystal elasticity measurements within the diopside-jadeite solid solution indicates that the linear trends are valid for most C_{ij} values. The v_p and v_s of omphacite decrease with diopside content, though the velocity changes are small as diopside component exceeds 70%. We also found that both the isotropic v_p and v_s , as well as the seismic anisotropy of eclogite, changed strongly with the bulk-chemical composition. The relationship between the anisotropic velocities of eclogite and the chemical composition can be a useful tool to trace the origin of the eclogitic materials in the Earth's mantle.

Keywords: Clinopyroxene, Brillouin spectroscopy, elastic properties, jadeite

INTRODUCTION

Clinopyroxene (Cpx) is one of the major mineral phases in the Earth's upper mantle (Ringwood 1975; Anderson and Bass 1984). The chemical composition of the upper mantle Cpx is close to Fe-bearing diopside (Di, CaMgSi₂O₆), with significant jadeite (Jd, NaAlSi₂O₆) component (e.g., Nestola et al. 2016). The crust of the subducted slabs and the delaminated lithosphere from continental roots form eclogite at depth >70-100 km (Irifune et al. 1986; Kay and Kay 1993). Cpx constitutes up to 70% of natural eclogite. The Cpx in eclogite is essentially Fe-bearing omphacite, which is the solid solution between Di and Jd. The coupled substitution of (Ca, Mg) for (Na, Al) in the Di-Jd solid solution stiffens the crystal structure, which has been confirmed by both the high-pressure single-crystal X-ray diffraction experiments and the sound velocity measurements (Kandelin and Weidner 1988; Nestola et al. 2006; Sang et al. 2011; Pandolfo et al. 2012; Zhang et al. 2016). The bulk (K_s) and shear (G) moduli of the end-member Jd are ~25% and ~18% higher, respectively, than the end-member Di (Kandelin and Weidner 1988; Sang et al. 2011). In the Di-Jd solid solution, the chemical composition strongly influences the elastic properties and therefore, should be considered for modeling the seismic properties of pyrolite and eclogite.

The general chemical formula of Cpx is (M2M1)Si₂O₆. The M2 site is usually occupied by cations with larger ionic radii,

such as Ca^{2+} and Na^+ . The M1 site is slightly smaller, thus preferred by smaller cations, such as Mg^{2+} and Al^{3+} . At low-temperature conditions, the cations in the M1 and M2 sites are usually ordered, and the omphacite crystals show a lower P2/n symmetry, compared with the higher C2/c symmetry of the Di and Jd end-members. As temperature increases, the ordering of the cations degrades in both the M1 and M2 sites, and eventually, the ordered P2/n structure will convert to a completely disordered C2/c structure at temperatures higher than ~725 °C (Fleet et al. 1978; Carpenter 1980).

Previous high-pressure equation of state studies in the Di-Jd solid solution (e.g., Nestola et al. 2006; Pandolfo et al. 2012; Zhang et al. 2016) provided constraints to the compositiondependent isothermal bulk modulus (K_T) . However, determination of the seismic velocities and elastic anisotropy requires direct single-crystal sound velocity measurements. The single-crystal elastic properties of Cpx with close to upper mantle chemical compositions have been studied previously (Levien et al. 1979; Bhagat et al. 1992; Collins and Brown 1998; Isaak and Ohno 2003; Norris 2008; Sang et al. 2011; Walker 2012; Skelton and Walker 2015). Levien et al. (1979) first measured the single-crystal elasticity of the Di end-member using Brillouin spectroscopy, and the results were improved in a more recent study by Sang et al. (2011). Isaak and Ohno (2003) measured a Cr-bearing Di using resonant ultrasound spectroscopy, which agrees well with Sang et al. (2011), suggesting that the incorporation of small amounts of Cr has no resolvable effect on the elastic properties. A Cpx with more realistic and complicated upper mantle com-

viz site is usually occupied by cations with larger follic fault,

 $^{*\} E-mail: minghao@unm.edu\ (Orcid\ 0000-0003-1380-3569)\ and\ jinzhang@unm.edu\ (Orcid\ 0000-0003-3569)\ and\ jinzhang@unm.edu\ (Orcid\ 0000-0003-3569)\$

position was measured by Collins and Brown (1998) using the stimulated light scattering technique. They found some irregular trends that deviate from linear mixing models for C_{55} , C_{66} , and C_{35} . Omphacite has only once been measured at ambient condition by Bhagat et al. (1992). The sample used by Bhagat et al. (1992) is Jd-rich, whereas no single-crystal elasticity measurements are available for the Di-rich omphacites. Walker (2012) and Skelton and Walker (2015) theoretically determined the C_{ij} values of Di, Jd, and Di₅₀Jd₅₀ at 0 K using density functional theory calculations. They found that the linear mixing model did not work for C_{11} , C_{12} , C_{13} , and C_{23} . However, it remains unknown whether their conclusion still holds at temperatures higher than 0 K.

To improve our understanding of the single-crystal elastic properties of omphacite in the Di-Jd solid solution, we have measured the elastic properties of a C2/c Jd and a P2/n Di-rich omphacite at ambient condition. The accuracy and precision of the single-crystal Brillouin spectroscopy measurements are much better compared to several decades ago (Zhang et al. 2011; Bass and Zhang 2015). Employing the new results obtained in this study, we reanalyzed the elastic properties of the Di-Jd solid solution and explored the compositional effects on the seismic properties of eclogite over a wide compositional range.

EXPERIMENTAL METHODS

The compositions of the natural Jd and omphacite samples were measured by electron probe microanalysis (EPMA), using the JEOL 8200 Electron Microprobe facility hosted by the Institute of Meteoritics at University of New Mexico (UNM). Approximately 1 mm size crystals were polished and used for EPMA analysis, operating at 15 kV accelerating voltage and 20 nA beam current. The element standards were albite for Na, forsterite for Mg, almandine for Al and Fe, diopside for Si and Ca. Oxygen was calculated by stoichiometry from the cations. The detailed analysis results are summarized in Table 1. Normalizing the chemical analysis in terms of Di and Jd yields simplified compositions of Di_{3.2}Jd_{96.8} for the Jd sample and Di_{70.5}Jd_{29.5} for the omphacite sample. The crystals were then double-side polished into pellets with ~15 μ m thickness. They were scratch-free and inclusion-free under optical examination.

The unit-cell parameters and crystallographic orientations for all samples were determined by single-crystal X-ray diffraction at GeoSoilEnviroCARS experimental station 13-BM-D, Advanced Photon Source, Argonne National Laboratory. The X-ray was monochromated to 37.0 keV and focused to 3-4 × 7-8 μm . A stationary Perkin-Elmer image plate was used as the detector. Diffraction images were collected at 1 °/step for the ±16° opening and the exposure time was 5 s/°. The obtained unit-cell parameters are: a=9.439(5), b=8.883(4), c=5.228(1) Å, $\beta=107.50(2)^\circ$, and $V_0=404.0(3)$ ų [density $\rho=3.302(5)$ g/cm³] for Di₁₂Jd₉₆₈; a=9.632(3), b=8.843(3), c=5.245(1) Å, $\beta=106.31(2)^\circ$, and $V_0=428.8(2)$ ų [density $\rho=3.339(2)$ g/cm³] for Di_{70.5}Jd_{29.5}. The space groups are also confirmed to be C2/c and P2/n for the Jd and omphacite sample, respectively.

For each sample, we used three different orientations for the single-crystal Brillouin spectroscopy measurements. The face normals of the measured samples are: (-0.692, 0.714, -0.106), (0.116, 0.993, -0.021),and (-0.043, 0.130, -0.999) for $Di_{3.2}Jd_{96.8}$; (-0.044, 0.979, 0.197), (0.242, 0.299, -0.923), and (0.697, 0.717, -0.016) for $Di_{70}Jd_{295}$. The accuracy of the measured plane normals is 0.5° or better.

The Brillouin spectroscopy experiments were performed in the high-pressure

TABLE 1. The chemical composition of the Cpx samples used in this study

Elements	Di _{70.5} Jd _{29.5} (wt%)	Di _{3.2} Jd _{96.8} (wt%)
Na ₂ O	4.13	14.65
MgO	11.77	0.42
AI_2O_3	7.59	24.42
SiO ₂	54.73	59.62
CaO	17.59	0.81
FeO	3.59	0.69
Total	99.42	100.62

laser spectroscopy laboratory at UNM. We used a 300 mW 532 nm single-mode diode-pumped solid-state laser as the light source. The measurements were carried out using a 50° symmetric forward scattering geometry. The scattering angle was calibrated to be 50.37(5)° using a standard silica glass Corning 7980 (Zhang et al. 2011, 2015). For each crystal, shear velocities (ν_a) and compressional velocities (ν_p) were measured at 13 different χ angles (0, 30, 60, 90, 120, 150, 180, 195, 225, 255, 285, 315, 345) along the 360° azimuth to avoid any geometrical errors. All Brillouin spectra are with excellent signal-to-noise ratios. A typical Brillouin spectrum is shown in Figure 1.

RESULTS AND DISCUSSION

A least-square inversion of the Christoffel equation was used to calculate the best-fit values for the 13 independent C_{ij} values at ambient condition (Weidner and Carleton 1977). The measured velocities associated with the velocity model predicted by the C_{ij} model of Jd are shown in Figure 2. The ambient $K_{\rm S}$ and G were calculated using the Voigt-Reuss-Hill (VRH) averaging scheme (Hill 1963). The $K_{\rm S}$ and G are 138(3) and 84(2) GPa for Di_{3.2}Jd_{96.8}, and 123(3) and 73(2) GPa for Di_{70.5}Jd_{29.5}, respectively.

Table 2 shows a complete list of the C_{ij} values obtained in this study alongside with both the results of the end-member Jd measured by Kandelin and Weidner (1988), and those of the Jd-rich omphacite determined by Bhagat et al. (1992). The C_{ij} values of the $\mathrm{Di}_{3.2}\mathrm{Jd}_{96.8}$ sample measured in this study are in general agreement, yet with much smaller uncertainties, compared with Kandelin and Weidner (1988). The small amount of the Di component in our Jd sample may explain the smaller C_{12} and K_S determined in this study. As expected, most C_{ij} values of the $\mathrm{Di}_{70.5}\mathrm{Jd}_{29.5}$ sample measured in this study are smaller than the values of the $\mathrm{Di}_{34.1}\mathrm{Jd}_{65.9}$ omphacite measured by Bhagat et al. (1992).

Figure 3 shows the elastic moduli change as a function of chemical composition in the Di-Jd solid solution (Kandelin and Weidner 1988; Bhagat et al. 1992; Collins and Brown 1998; Isaak and Ohno 2003; Sang et al. 2011). We have utilized the following empirical polynomial function to describe the compositional dependence of the elastic moduli:

$$E = a_0 + a_1 \times c + a_2 \times c^2 \tag{1}$$

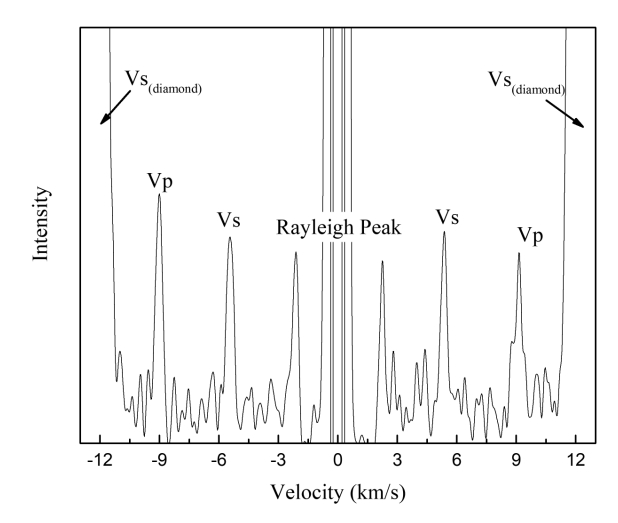


FIGURE 1. A typical the Brillouin spectrum showing one v_s and one v_p from the sample.

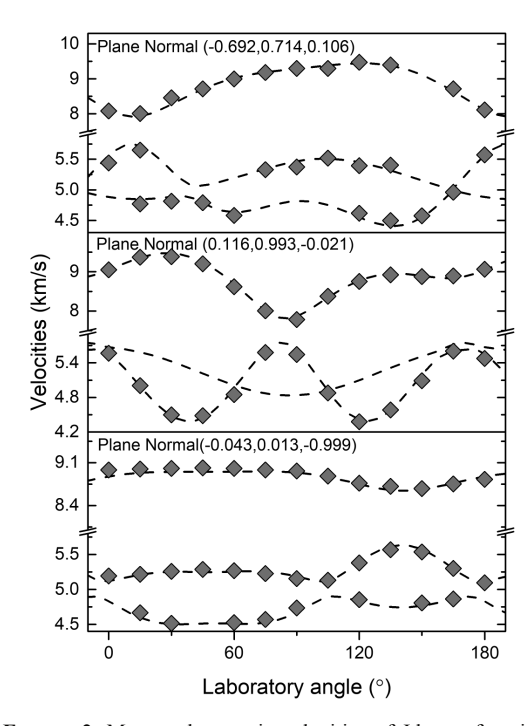


FIGURE 2. Measured acoustic velocities of Jd as a function of laboratory χ angles within the sample plane. Dashed lines are the acoustic velocities calculated from the best-fit single-crystal elasticity model; diamonds are the experimentally determined velocities. Errors are within the size of the symbols.

where E represents the elastic properties, including the C_{ii} values, $K_{\rm S}$, and G; c is the proportion of the Di component in the Di-Jd solid solution; a_0 , a_1 , and a_2 are the fitting parameters shown in Table 3. The red-shaded regions in Figure 3 represent the 95% confidence intervals. Similar to the negative correlation between the Di content and the K_T determined by previous X-ray diffraction experiments, the directly measured $K_{\rm S}$ and G linearly decrease with the Di content as well. Actually, all single-crystal elastic moduli show close-to-linear relationships with the Jd and Di content, except C_{13} and C_{23} . The C_{13} and C_{23} of omphacite are slightly higher and lower, respectively, than the predicted values from linear mixing models. The omphacite sample we measured is Cr-free. In Figure 3, most of the elastic moduli measured by Isaak and Ohno (2003) are actually within the shaded 95% confidence intervals. This confirms that a small amount of Cr does not have a noticeable influence on the elastic properties of Di as reported by Sang et al. (2011). It is also worth noting that the C_{33} , C_{55} , and C_{35} values of the sample measured by Collins and Brown (1998) lie outside the trends determined from other measurements, which may be explained by the high Tschermak's content (12 mol%) of the sample measured by Collins and Brown (1998).

Skelton and Walker (2015) theoretically calculated the elastic properties of $Di_{50}Jd_{50}$ omphacite and compared with Walker (2012) to investigate the elasticity change within the Di-Jd solid solution at 0 K. They found out that the C_{11} , C_{12} , C_{13} , and C_{23} of omphacite were off from the linear mixing trend of Di and Jd. In this study, the C_{13} and C_{23} of omphacite are indeed slightly

TABLE 2. Single-crystal elastic properties of different Cpx samples at ambient condition

	Jd		Omphacite		
ρ (g/cm³)	3.302(5)	3.33	3.339(2)	3.327(2)	
composition	$Di_{3.2}Jd_{96.8}$	Jd	$Di_{70.5}Jd_{29.5}$	$Di_{34.1}Jd_{65.9}$	
	This study	Kandelin and	This study	Bhagat et al. (1992)	
		Weidner (1988)			
C ₁₁ (GPa)	265.4(9)	274(4)	231.7(8)	257(1)	
C_{22} (GPa)	247(1)	253(4)	202(1)	216.2(8)	
C_{33} (GPa)	274(1)	282(3)	255.2(9)	260.2(7)	
C ₄₄ (GPa)	85.8(7)	88(2)	78.4(5)	80.2(6)	
C_{55} (GPa)	69.3(5)	65(4)	68.9(5)	70.6(4)	
C_{66} (GPa)	93.0(7)	94(2)	73.6(4)	85.8(5)	
C_{12} (GPa)	85(1)	94(2)	85(1)	86(1)	
C_{13} (GPa)	66(1)	71(8)	77(1)	76(1)	
C_{23} (GPa)	87(2)	82(4)	58(2)	71(1)	
C_{15} (GPa)	5.4(7)	4(3)	7.8(5)	7.1(6)	
C_{25} (GPa)	17(1)	14(4)	6(1)	13(1)	
C_{35} (GPa)	28.7(6)	28(3)	39.5(5)	33.7(8)	
C_{46} (GPa)	14.6(6)	13(1)	6.3(4)	10.2(3)	
K_S^R (GPa)	135.9(7)	141(2)	119.7(6)	128.0(5)	
G^R (GPa)	82.7(3)	83(2)	72.0(3)	77.7(2)	
K_s^V (GPa)	140.1(7)	145(2)	125.3(6)	133.5(5)	
G^{V} (GPa)	86.3(3)	87(1)	75.5(3)	80.6(2)	
K_s (GPa)	138(3)	143(2)	122(3)	130.8(5)	
G (GPa)	84(2)	85(2)	74(2)	79.2(2)	
V_p (km/s)	8.71(4)	8.77(5)	8.13(4)	8.43(4)	
$V_{\rm s}$ (Km/s)	5.06(3)	5.05(5)	4.70(3)	4.88(3)	
RMS error (m/s	42.2	\	38.8	49	

Note: The superscripts R and V refer to the Reuss and Voigt bounds of the homogeneous isotropic aggregate under VRH averaging scheme.

higher and lower than the values predicted by the linear mixing model. However, the C_{11} and C_{12} actually agree well (Fig. 3). The difference between this study and Skelton and Walker (2015) may result from the temperature difference. Our measurements were carried out at room temperature, whereas their calculation was performed at 0 K. Skelton and Walker (2015) suggested that the differential cation ordering between the M1 site and M2 site in omphacite caused the nonlinear mixing. In particular, the cations in the M2 site are more disordered than M1 at low temperatures. Elevating the temperature would disorder the cations within the crystal structure and result in a close to linear mixing trend. This might explain the absence of the nonlinear mixing trend in C_{11} and C_{12} observed in this study. The differences between the measured values and the predicted linear mixing values of C_{13} and C_{23} are also smaller than what was calculated by Skelton and Walker (2015). Further computational investigations at room-temperature condition can help us quantitatively understand the differences between this experimental study and previous theoretical investigations, as well as critically evaluate our explanations above.

GEOPHYSICAL IMPLICATIONS

Based on the measured single-crystal elastic properties, we calculated the aggregate v_s and v_p within the Di-Jd solid solution (Fig. 4a). Both the v_p and v_s display a nonlinear decrease with the Di content. The composition induced velocity change is negligible as the Di component exceeds 70%.

The Jd component of omphacite in natural eclogite varies from ~10 to ~65% (e.g., Coleman et al. 1965; Smyth et al. 1991; Bhagat et al. 1992). Based on the compositional dependence of the omphacite velocities obtained in this study, and the existing sound velocity measurements of garnets (Sinogeikin and Bass 2002; Gwanmesia et al. 2014; Arimoto et al. 2015), we

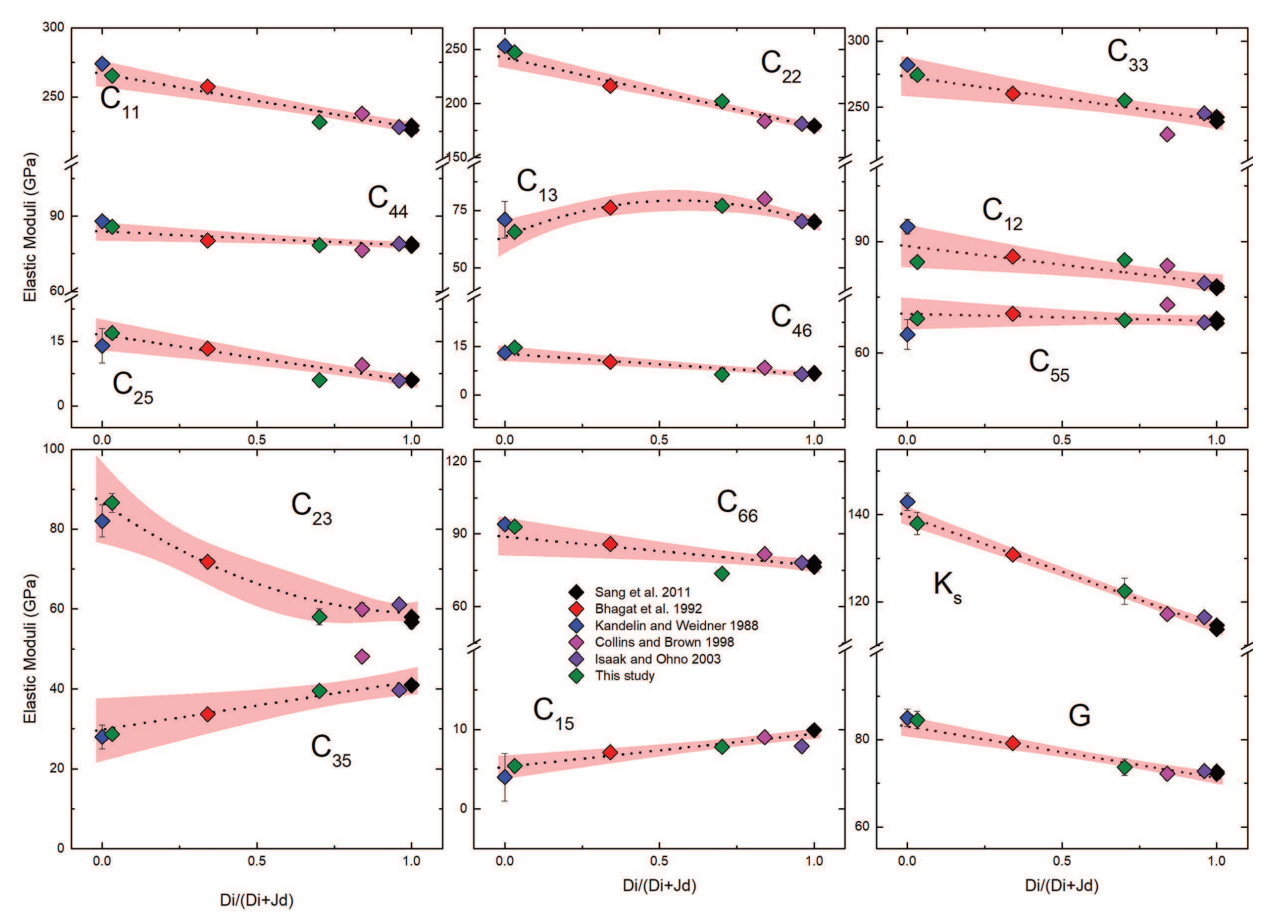


FIGURE 3. C_{ij} values, K_{S_i} and G as a function of chemical composition in the Di-Jd solid solution. The light red shaded regions represent the 95% confidence intervals. (Color online.)

TABLE 3. Polynomial fitting results for the compositional dependence of elastic moduli of the Di–Jd solid solution; a_0 , a_1 , and a_2 are defined in Equation 1

are defined in Equation 1				
Elastic moduli	a_0	a_1	a_2	
C ₁₁ (GPa)	267(4)	-39(4)	0	
C ₂₂ (GPa)	243(4)	-64(4)	0	
C ₃₃ (GPa)	273(6)	-33(7)	0	
C ₄₄ (GPa)	84(1)	-5(2)	0	
C ₅₅ (GPa)	71(2)	-2(2)	0	
C ₆₆ (GPa)	89(4)	-12(4)	0	
C ₁₂ (GPa)	89(2)	-10(3)	0	
C ₁₃ (GPa)	64(3)	56(12)	-50(10)	
C ₂₃ (GPa)	87(4)	-53(16)	26(13)	
C ₁₅ (GPa)	5.3(7)	4.2(9)	0	
C ₂₅ (GPa)	17(1)	-11(2)	0	
C ₃₅ (GPa)	30(3)	12(4)	0	
C_{46} (GPa)	12.8(9)	-6(1)	0	
K_s (GPa)	139.7(8)	-26(1)	0	
G (GPa)	83.1(9)	-12(1)	0	

calculated the v_p and v_s of three different eclogites at ambient condition assuming the Voigt averaging scheme (Table 4, Coleman et al. 1965; Voigt 1889). The v_p and v_s of eclogite increase with the Jd component in omphacite. In particular, the v_p and v_s differences between the eclogite 1 and 3 are as large as 3%. The bulk-chemical composition of eclogite depends on its parent rock. If the parent rock of eclogite has a strong continental and/or sediment component, the omphacite in eclogite will be enriched in Na and Al, and thus high in Jd content (Irifune et al. 1994).

The relationship between the absolute velocities of eclogite and the chemical composition can be a useful tool to trace the origin of the eclogitic materials in the mantle.

Due to the elastically isotropic nature of the garnet, omphacite is the major anisotropy contributor in eclogite. Thus, to study the anisotropic seismic properties of eclogite, it is important to investigate the composition-dependent elastic anisotropy in the Di-Jd solid solution.

In this study, universal anisotropy index (A^U) , azimuthal v_p anisotropy (A^{v_p}) , and radial v_s anisotropy (D^{v_s}) are calculated in the Di-Jd solid solution.

 A^U is used as a measure of the overall elastic anisotropy for materials with arbitrary symmetry (Ranganathan and Ostoja-Starzewski 2008):

$$A^{U} = 5\frac{G^{V}}{G^{R}} + \frac{K_{S}^{V}}{K_{S}^{R}} - 6 \tag{2}$$

where the superscripts R and V refer to the Reuss and Voigt bounds of the homogeneous isotropic aggregate under VRH averaging scheme.

 A^{vp} represents the maximum velocity difference of all v_p propagating along different directions:

$$A^{v_p} = \frac{v_{\text{p,max}} - v_{\text{p,min}}}{v_{\text{p}}} \tag{3}$$

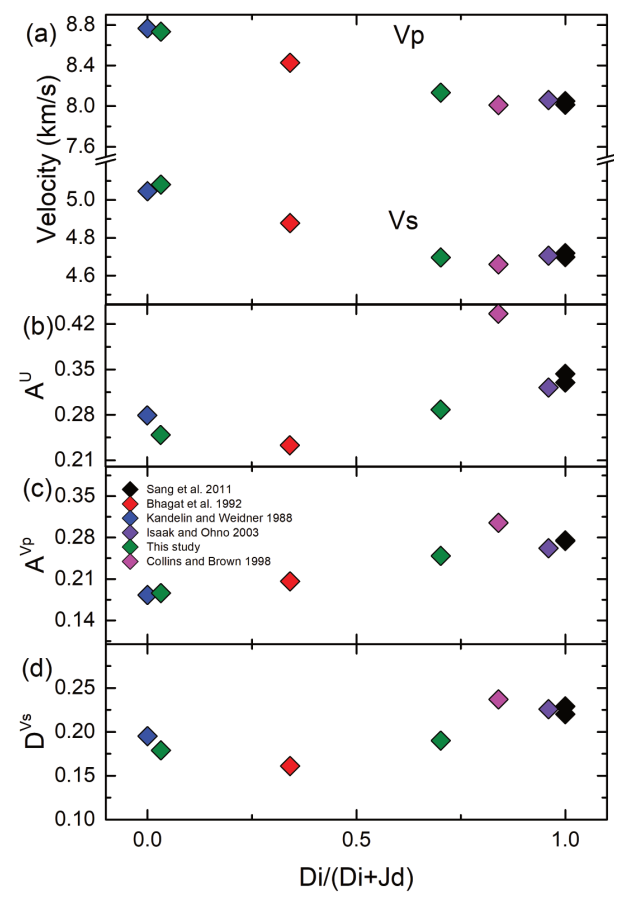


FIGURE 4. The velocities, A^U , A^{vp} , and D^{vs} as a function of chemical composition. (Color online.)

TABLE 4. The end-member mineral proportions, and calculated v_p and v_v for the three eclogite samples

and tyre, the times established					
		Eclogite 1	Eclogite 2	Eclogite 3	
Omphacite	Jd	10.5%	21.0%	45.5%	
	Di	59.5%	49.0%	24.5%	
Garnet	Pyrope	20.1%	13.5%	4.8%	
	Grossular	3.6%	4.8%	6.9%	
	Almandine	5.7%	11.7%	18.3%	
v_s (km/s)		4.76	4.79	4.90	
v_p (km/s)		8.26	8.36	8.51	

Note: We assume the volume proportions of omphacite and garnet are 70% and 30%, respectively, for all three eclogites.

 D^{vs} , which describes the maximum velocity difference between the two orthogonally polarized shear waves propagating along the same direction, is defined as:

$$D^{v_{s}} = \frac{\left| v_{S_{1}} - v_{S_{2}} \right|_{\text{max}}}{v_{S}}.$$
 (4)

Figures 4b, 4c, and 4d show variations of the anisotropy indices as a function of chemical composition in the Di-Jd solid solution. The calculated anisotropy indices, especially the A^U and A^{rp} , of the Cpx sample measured by Collins and Brown (1998), lie outside the trends determined from all the other studies. This again may be explained by its high Tschermak's content

(12mol%). The Di end-member has the highest A^U , A^{vp} , and A^{vs} within the Di-Jd solid solution. The A^{vp} decreases linearly as the Jd component increases. The A^{vp} of the Di end-member is 60% higher than that of the Jd end-member. The trends in D^{vs} and A^U are not as clear. Jd-rich omphacite seems to have similar D^{vs} and A^U as Jd. Nevertheless, the enrichment of Jd component in omphacite is likely to decrease the overall elastic anisotropy of Cpx. The single-crystal elasticity data presented in this study can serve as the basis for future anisotropy modeling based on the lattice preferred orientation of the omphacite crystals in natural eclogite within a wide range of chemical compositions (Zhang et al. 2006; Zhang and Green 2007).

FUNDING

This work is supported by the National Science Foundation (NSF) under Grant EAR 1646527 (J.Z.) and the start-up fund from UNM (J.Z.). This research used resources of the APS, a U.S. DOE Office of Science User Facility operated for the DOE Office of Science by Argonne National Laboratory under Contract No. DE-AC02-06CH11357.

ACKNOWLEDGMENTS

The authors thank Jane Silverstone (UNM) and Jay Bass (UIUC) for providing the samples used in this study; Mike Spilde for the help with EPMA experiment at the Institute of Meteoritics at UNM.

REFERENCES CITED

Anderson, D.L., and Bass, J.D. (1984) Mineralogy and composition of the upper mantle. Geophysical Research Letters, 11, 637–40.

Arimoto, T., Gréaux, S., Irifune, T., Zhou, C., and Higo, Y. (2015) Sound velocities of Fe₃Al₂Si₃O₁₂ almandine up to 19 GPa and 1700 K. Physics of the Earth and Planetary Interiors, 246, 1–8.

Bass, J.D., and Zhang, J.S. (2015) Techniques for measuring high P/T elasticity. Schubert, Oxford.

Bhagat, S.S., Bass, J.D., and Smyth, J.R. (1992) Single-crystal elastic properties of omphacite-C2/c by Brillouin spectroscopy. Journal of Geophysical Research: Solid Earth, 97, 6843–6848.

Carpenter, M.A. (1980) Mechanisms of exsolution in sodic pyroxenes. Contributions to Mineralogy and Petrology, 71, 289–300.

Coleman, R.G., Lee, D.E., Beatty, L.B., and Brannock, W.W. (1965) Eclogites and eclogites: their differences and similarities. Geological Society of America Bulletin, 76, 483–508.

Collins, M.D., and Brown, J.M. (1998) Elasticity of an upper mantle clinopyroxene. Physics and Chemistry of Minerals, 26, 7–13.

Fleet, M.E., Herzberg, C.T., Bancroft, G.M., and Aldridge, L.P. (1978) Omphacite studies: I. The $P2/n \rightarrow C2/c$ transformation. American Mineralogist, 63, 1100–1106.

Gwanmesia, G.D., Wang, L., Heady, A., and Liebermann, R.C. (2014) Elasticity and sound velocities of polycrystalline grossular garnet (Ca₃Al₂Si₃O₁₂) at simultaneous high pressures and high temperatures. Physics of the Earth and Planetary Interiors, 228, 80–87.

Hill, R. (1963) Elastic properties of reinforced solids: some theoretical principles. Journal of the Mechanics and Physics of Solids, 11, 357–372.

Irifune, T., Sekine, T., Ringwood, A.E., and Hibberson, W.O. (1986) The eclogite-garnetite transformation at high pressure and some geophysical implications. Earth and Planetary Science Letters, 77, 245–256.

Irifune, T., Ringwood, A.E., and Hibberson, W.O. (1994) Subduction of continental crust and terrigenous and pelagic sediments: an experimental study. Earth and Planetary Science Letters, 126, 351–368.

Isaak, D.G., and Ohno, I. (2003) Elastic constants of chrome-diopside: application of resonant ultrasound spectroscopy to monoclinic single-crystals. Physics and Chemistry of Minerals, 30, 430–439.

Kandelin, J., and Weidner, D.J. (1988) The single-crystal elastic properties of jadeite. Physics of the Earth and Planetary Interiors, 50, 251–260.

Kay, R.W., and Kay, S.M. (1993) Delamination and delamination magmatism. Tectonophysics, 219, 177–189.

Levien, L., Weidner, D.J., and Prewitt, C.T. (1979) Elasticity of diopside. Physics and Chemistry of Minerals, 4, 105–113.

Nestola, F., Boffa Ballaran, T., Liebske, C., Bruno, M., and Tribaudino, M. (2006) High-pressure behaviour along the jadeite NaAlSi₂O₆-aegirine NaFeSi₂O₆ solid solution up to 10 GPa. Physics and Chemistry of minerals, 33, 417–425.

Nestola, F., Alvaro, M., Casati, M.N., Wilhelm, H., Kleppe, A.K., Jephcoat, A.P., Domeneghetti, M.C., and Harris, J.W. (2016) Source assemblage types for cratonic diamonds from X-ray synchrotron diffraction. Lithos, 265, 334–338.

- Norris, S. (2008) Elastic properties of jadeite. Undergraduate Senior thesis, University of Illinois.
- Pandolfo, F., Nestola, F., Cámara, F., and Domeneghetti, M.C. (2012) New ther-moelastic parameters of natural C2/c omphacite. Physics and Chemistry of Minerals, 39, 295–304.
- Ranganathan, S.I., and Ostoja-Starzewski, M. (2008) Universal elastic anisotropy index. Physical Review Letters, 101, 055504.
- Ringwood, A.E. (1975) Composition and Petrology of the Earth's Mantle.

 McGraw-Hill
- Sang, L., Vanpeteghem, C.B., Sinogeikin, S.V., and Bass, J.D. (2011) The elastic properties of diopside, CaMgSi₂O₆. American Mineralogist, 96, 224–227.
- Sinogeikin, S.V., and Bass, J.D. (2002) Elasticity of majorite and a majorite-pyrope solid solution to high pressure: Implications for the transition zone. Geophysical Research Letters, 29, 4–1.
- Skelton, R., and Walker, A.M. (2015) The effect of cation order on the elasticity of omphacite from atomistic calculations. Physics and Chemistry of Minerals, 42, 677–691.
- Smyth, J.R., Bell, D.R., and Rossman, G.R. (1991) Incorporation of hydroxyl in upper-mantle clinopyroxenes. Nature, 351, 732.
- Voigt, W. (1889) Ueber die Beziehung zwischen den beiden Elasticitätsconstanten isotroper Körper. Annalen der physik, 274, 573–587.
- Walker, A.M. (2012) The effect of pressure on the elastic properties and seismic anisotropy of diopside and jadeite from atomic scale simulation. Physics of the Earth and Planetary Interiors, 192, 81–89.

- Weidner, D.J., and Carleton, H.R. (1977) Elasticity of coesite. Journal of Geophysical Research, 82, 1334–1346.
- Zhang, J., and Green, H.W. (2007) Experimental investigation of eclogite rheology and its fabrics at high temperature and pressure. Journal of Metamorphic Geology, 25, 97–115.
- Zhang, J., Green, H.W. II, and Bozhilov, K.N. (2006) Rheology of omphacite at high temperature and pressure and significance of its lattice preferred orientations. Earth and Planetary Science Letters, 246, 432–443.
- Zhang, J.S., Bass, J.D., Taniguchi, T., Goncharov, A.F., Chang, Y.Y., and Jacobsen, S.D. (2011) Elasticity of cubic boron nitride under ambient conditions. Journal of Applied Physics, 109, 063521.
- Zhang, J.S., Bass, J.D., and Zhu, G. (2015) Single-crystal Brillouin spectroscopy with CO₂ laser heating and variable q. Review of Scientific Instruments, 86, 063905
- Zhang, D., Hu, Y., and Dera, P.K. (2016) Compressional behavior of omphacite to 47 GPa. Physics and Chemistry of Minerals, 43, 707–715.

MANUSCRIPT RECEIVED FEBRUARY 2, 2019 MANUSCRIPT ACCEPTED APRIL 7, 2019 MANUSCRIPT HANDLED BY JENNIFER KUNG